by the expression

$$1/m_{\rm op}^*=\frac{1}{N}\sum_k n_k/m^*(k)\,, \tag{4.2}$$

where n_k is the Fermi distribution, N is the number of conduction electrons per unit volume, and $f_{k'k}$ is the "oscillator strength" for transitions from state k to state k';

$$f_{k'k}=\frac{2\hbar}{m\omega_{k'k}}\left|\int \chi_{k'}^*\nabla\chi_k d^3\mathbf{r}\right|^2, \tag{4.3}$$

where $\hbar\omega_{k'k}$ is the energy difference between the Bloch states χ_k and $\chi_{k'}$. From the expression (2.17) which defines $g_{k'kQ\lambda}$ in the limit as $Q\to 0$, we obtain

$$\langle\chi_{k'}|\nabla|\chi_k\rangle=i[\mathbf{k}'\langle\mathbf{k}'|\tilde{W}(k)|\mathbf{k}\rangle -\mathbf{k}\langle\mathbf{k}|\tilde{W}(k')|\mathbf{k}'\rangle^*]/\hbar\omega_{k'k}\,, \tag{4.4}$$

where $\hbar\omega_{k'k}=\epsilon_{k'}-\epsilon_k$. The present formalism can therefore be used to evaluate oscillator strength directly in nearly-free-electron metals without recourse to energy-band calculations. However, the pseudopotential needed is different from that determining, for example, electron-phonon interaction and the energy-band structure. In addition, (4.4) can be evaluated self-consistently by replacing $\tilde{W}$ and $\tilde{W}_{\rm eff}$ given by (3.18).

For the complete problem we have, in general, a Green's function

$$G(k,\tilde{E})=1/[\tilde{E}-E_k-\textstyle\sum(k,\tilde{E})], \tag{4.5}$$

where $\sum(k,\tilde{E})$ is the self-energy, so that we can define an effective "electromagnetic" mass by

$$(1/\hbar)\partial\tilde{E}/\partial k|_{k=k_F}=\hbar k_F/m_{\rm e-m}^*, \tag{4.6}$$

and find, from the poles of (4.5),

$$m_{\rm e-m}^*=m_B(1-\partial\textstyle\sum/\partial\tilde{E})|_{k=k_F}, \tag{4.7}$$

where m_B is the zero-field Bloch effective mass. This is our effective-mass theorem. This is the analog of the so-called "thermal" mass in the electron-phonon interaction.[16] It does not seem at the present time to have any more general meaning than the optical effective mass introduced above. But it is evidently the proper mass to be used in describing the influence of the field on the dynamical properties of the Bloch electron. No attempt will be made here to compute this mass explicitly; in practice, it should follow the procedure for the electron-phonon case exactly.[16]

ACKNOWLEDGMENTS

I wish to thank Robert Shaw for a critical reading of the manuscript.

[16] See, e.g., A. O. E. Animalu, F. Bonsignori, and V. Bortolani, Nuovo Cimento **44B**, 83 (1966).

PHYSICAL REVIEW VOLUME 163, NUMBER 3 15 NOVEMBER 1967

Fermi Surface of Lead from Kohn Anomalies

R. STEDMAN, L. ALMQVIST,* G. NILSSON, AND G. RAUNIO*
AB Atomenergi, Studsvik, Nyköping, Sweden
(Received 16 June 1967)

The dispersion relations for phonons in lead determined by neutron spectrometry exhibit a large number of Kohn anomalies, which may all be related to the Fermi surface in a consistent manner by considering both electron transitions diametrically across the Fermi surface and nondiametral transitions between points with parallel tangent planes. Factors affecting the size and shape of anomalies are reviewed. The detailed interpretation of anomalies leads to a mapping of the Fermi surface, and the result may be compared with that of Anderson and Gold, who used the de Haas–van Alphen method. There is fair agreement, with significant particular differences. The sizes of anomalies have been interpreted in terms of a screened ion-electron interaction.

1. INTRODUCTION

SINCE Kohn[1] pointed out that the phonon-electron interaction changes abruptly along surfaces in the wave-vector space of phonons which are directly related to the Fermi surface, and that this change may be observable as kinks in phonon dispersion curves, such anomalies have been observed in some metals. Brockhouse *et al.*[2] were the first to see the effect, in lead. As they pointed out, the investigation of the Fermi surface via phonons and neutrons is a potentially interesting complement to other methods. The neutron method does not require particularly pure samples or low temperatures, and the interpretation of data is mostly just a matter of geometrical constructions. But it is rather elaborate and, with present neutron sources and spectrometers, applicable only to metals that exhibit relatively large anomalies and are especially amenable to neutron spectrometry, and in fact has not previously been used for a comprehensive study of a Fermi surface. The anomalies in lead seemed to be sufficiently pro-

* Chalmers University of Technology, Gothenburg, Sweden.
[1] W. Kohn, Phys. Rev. Letters **2**, 393 (1959).
[2] B. N. Brockhouse, K. R. Rao, and A. D. B. Woods, Phys. Rev. Letters **7**, 93 (1961).

TABLE I. The sizes and senses of Kohn anomalies for a nearly spherical Fermi surface. Numbering is in the order of increasing q according to Fig. 1. A plus sign indicates that the anomaly is upward in the direction of increasing q, a minus sign the opposite. Brackets indicate that values are subject to considerable reservations.

Anomaly No.	$\Delta\omega$ (10^{13} rad sec^{-1}) L	T_1	T_2
[1,1,1]			
1	−0.025	−0.011	
2	+0.022	+0.009	
3	+0.012	0	
[2,0,0]			
1	(−0.010)	(−0.016)	
2	+0.014	0	
3	(−0.009)	(−0.014)	
4	−0.034	−0.016	
[2,2,0]			
1	−0.017	0	0
2	+0.017	0	+0.019
3	+0.019	+0.005	0
4	(−0.016)	0	(−0.014)
5	(−0.004)	(−0.013)	(−0.013)
6	(−0.004)	(−0.016)	(−0.013)
7	(−0.016)	0	(−0.014)
8	(−0.008)	(−0.008)	0
9	(−0.008)	(−0.009)	0

nounced to allow such an investigation, and to this end we carried out extensive measurements, both in symmetry directions and elsewhere. Many anomalies were revealed, some of which correspond directly to points on the Fermi surface on or near the symmetry axes, while others required for their interpretation detailed consideration of the surface topography. Twenty points on the Fermi surface could be assigned, amounting to a fairly complete determination of the whole surface. Our version is generally quite close to that of Anderson and Gold,[3] who used the de Haas–van Alphen method, but there are significant differences, particularly in the third zone.

2. FACTORS AFFECTING ANOMALIES

Kohn anomalies are associated with a small negative contribution to phonon energies due to virtual excitation of electrons by phonons, and occur because this contribution varies more or less abruptly when there is abrupt variation in the density of electron transitions with respect to wave-vector space. The important transitions are between states close to the Fermi surface so that the interaction condition $\mathbf{Q}=\mathbf{k}_1-\mathbf{k}_2$ (where $\mathbf{Q}$ is the unreduced phonon wave vector and $\mathbf{k}_1$, $\mathbf{k}_2$ are electron wave-vectors) may be regarded as a relation for points $\mathbf{k}_1$ and $\mathbf{k}_2$ on the Fermi surface. Abrupt variations of the transition density occur for pairs of points where the tangent planes are parallel. Diametrically opposite points on a sphere are an idealized example: Transition vectors parallel to the diameter and of length Q join small circles of the sphere which shrink as Q increases and disappear when $Q=2k_F$, so that the density of transitions falls from a constant value when Q is smaller than the limit $2k_F$ (if zones of thickness ΔQ are considered) to zero beyond the limit. When the sum of all possible transitions with their different energy transfers is taken into account, the anomaly is not so sharp as simple consideration of momentum transfer on the Fermi surface indicates, but there is still an upward shift of phonon frequency as Q increases through $2k_F$. If the surface is locally concave outwards, the shift is downward instead.

The rules that the sense of an anomaly is determined by the local curvature and that small curvature tends to make an anomaly large are inadequate when opposing tendencies are of comparable strength, e.g., at a saddle point with approximately equal and opposite principal curvatures. In such cases, definite conclusions cannot be reached merely by considering the shape of the surface: It may be that not only the curvature but also the variation of $\mathrm{grad}_k E$ (where E is electron energy) differs in different surface directions from the point concerned. If an anomaly is regarded as the sum of contributions from narrow segments of the Fermi surface that radiate from the point concerned, the contribution from each segment must take account of the variation in $\mathrm{grad}_k E$ as well as the curvature. Complications in this respect are particularly likely to occur near the intersections of the Fermi surface with Bragg planes.

Considerations of local shape are easily extended to transitions between points that are not diametrically opposite; in this case the shape to be considered is that of a surface which is given by the difference between the two local surfaces, taken along lines parallel to the chord between the points with parallel tangent planes.

The treatment of Kohn anomalies by Taylor[4] includes the angle between the transition vector and the normal to the Fermi surface. When this angle approaches 90°, anomalies become small. Such an angular dependence is at least partly included in our "difference surface," since the curvature of this surface increases as the angle concerned increases. Fuller consideration of this point is unnecessary here.

Taylor's formulas[4] include the effect of $\mathrm{grad}_k E$, i.e., the electron velocity v. (As they stand, the formulas are not symmetric in $\mathbf{v}_1$ and $\mathbf{v}_2$, but such symmetry would be introduced by a condition of inversion symmetry on the Fermi surface.) The significant thing for our qualitative discussion is that anomalies increase in size as electron velocities decrease, roughly as $|\mathbf{v}_1-\mathbf{v}_2|^{-1}$. This factor is directly related to the energy difference between electron states in the denominator of the second-order energy shift for a phonon interacting with electrons. Two consequences are that transitions between points on the same side of the Fermi surface may be strong, because the electron velocities are nearly parallel, and that regions of the Fermi surface near

[3] J. R. Anderson and A. V. Gold, Phys. Rev. **139**, 1459 (1965).

[4] P. L. Taylor, Phys. Rev. **131**, 1995 (1963).

Bragg planes may be particularly active, because the component of the electron velocity perpendicular to the Bragg plane is small.[5]

Other factors affecting the size of anomalies depend entirely on phonon quantities, and may be obtained from an equation expressing the variation of ω^2 with respect to q in a metal (see, for instance, Vosko *et al.*,[6] Eqs. 3.21, 5.1, 5.2):

$$\omega^2(\mathbf{q})=\omega_d^2(\mathbf{q})+\sum_{\mathbf{g}}((\mathbf{g}\cdot\mathbf{e}/g)^2F'(g)-(\mathbf{Q}\cdot\mathbf{e}/Q)^2F'(Q)) -(\mathbf{q}\cdot\mathbf{e}/q)^2F'(q), \quad (1)$$

where the sums do not include $\mathbf{g}=\mathbf{0}$. $\mathbf{Q}=\mathbf{q}+\mathbf{g}$, $\mathbf{q}$ being the phonon wave vector reduced to a cell near the origin of wave vector space and $\mathbf{g}$ a reciprocal lattice vector, and $\mathbf{e}$ is the unit polarization vector of the phonon. ω_d is associated with the direct interaction between ions, and F' with the interaction between ions via the conduction electrons. F' is explained in the text and diagrams of the article by Vosko *et al.*: It is the product of the square of an expression which refers to the interaction of a bare ion and an electron and a screening factor. Kohn anomalies are associated with a kink in this latter factor at $Q=2k_F$, the height of the kink being approximately 0.07 of the value of the function at this point, i.e., the kink in F' is about 0.07 of $F'(2k_F)$. Using the same units as Vosko *et al.*, the height of an anomaly ($\Delta\omega$) for a spherical Fermi surface should be approximately

$$\Delta\omega=0.035F'(2k_F)\cdot\omega_p^2(\mathbf{Q}\cdot\mathbf{e}/Q)^2\cdot(\text{symmetry factor})/\omega, \quad (2)$$

where ω_p is the plasma frequency (6.67×10^{13} rad sec^{-1} for lead), and the symmetry factor takes account of the number of simultaneous equal contributions to the sums of Eq. (1) which may occur when $\mathbf{q}$ is in a symmetry direction. Different models of the ion-electron interaction give values of $F'(2k_F)$ between 0.01 and 0.04. Departures of the Fermi surface from the spherical form will often make Eq. (2) quite inaccurate, but nevertheless it seems worthwhile using it for a first estimate of the expected sizes of anomalies, particularly since the relative sizes of the anomalies at the same position in different polarization branches should usually be given correctly by the formula. Table I shows the result of such a calculation, where for the sake of definiteness we have assumed $F'(2k_F)=0.01$, which is approximately the value for a Bardeen model (see Vosko *et al.*,[6] Fig. 21). Figure 1 explains the numbering of the anomalies: The quadrangle there is obtained by unfolding three sides of an elementary tetrahedral cell of reciprocal space, and the curves on it are the intersections with spheres of radius $2k_F$ (2.48 q units for the free-electron Fermi sphere in lead), centered at various lattice points, and slightly modified to indicate the effect that occurs near Bragg planes. Numbering is outward from the origin. The sign of an anomaly is plus in Table I if the anomaly is expected to be upward in the direction of increasing q in Fig. 1 (minus in the opposite case). The signs correspond to a spherical surface, neglecting the possible effect of Bragg planes on the shape of the Fermi surface in their neighborhood. The L branch in the table is always that with the highest frequency, the T_1 branch is next, and the T_2 branch the lowest; the only place where this may cause confusion is for $q>0.97$ in the [2,2,0] direction, where the branch with polarization in the [2,2,0] direction is the T_1 branch. Bracketed figures indicate that the shape of the Fermi surface at the point obviously departs considerably from the spherical form, so that these values are only of interest for the relation between the different branches.

Formula (2) may be inaccurate even for relative values of anomalies in different branches at the same position if the corresponding point on the Fermi surface is on a Bragg plane. This may be illustrated by reference to Fig. 4. From a consideration of the shape of the sur-

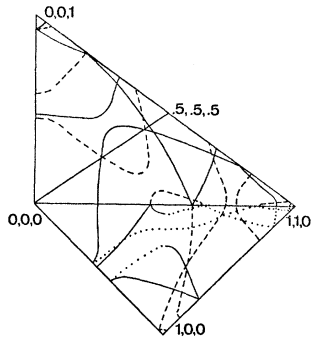

FIG. 1. Estimated positions of Kohn anomalies for a nearly spherical Fermi surface in planes between the principal symmetry directions.

[5] *Footnote added in manuscript.* L. M. Roth, H. J. Zeiger, and T. A. Kaplan [Phys. Rev. **149**, 519 (1966)] suggest that Taylor's results apply only to diametral transitions, and, moreover, that Kohn anomalies do not occur for transitions between parts of the Fermi surface where the normals are parallel (as distinct from antiparallel). The latter statement is of particular interest here, because two observed anomalies in the [1,1,1] dispersion curve have been interpreted by us in terms of electron transitions of the kind rejected by Roth *et al.* But it seems that their reasoning is incomplete in that they neglect the phonon energy in the denominators of their integrands [see their Eq. (24)], and when they point out that a certain integrand changes sign if $\mathbf{k}_1$ is exchanged for $-\mathbf{k}_2$, $\mathbf{k}_2$ for $-\mathbf{k}_1$ (i.e., when transitions with the same $\mathbf{Q}$ between opposite positions on the Fermi surface are considered) in order to draw the conclusion just mentioned about the parallel and antiparallel cases, they have omitted the accompanying change in the limits of integration in $\mathbf{k}$ space. Consideration of an example with transitions from an occupied region to the left of a point a on a line in $\mathbf{k}$ space to an unoccupied region to the right of a point b ($Q>b-a$) and transitions with the opposite regions occupied and unoccupied ($Q<b-a$) shows that there is no cancellation between the two groups of transitions. However, although the reason given by Roth *et al.* for the rejection of the "parallel" case does not seem acceptable, it is true that this case is not covered in Taylor's treatment, nor in our discussion in Sec. 2. A fuller treatment indicates that anomalies may occur in the "parallel" case, though they do not conform to the formulas we have used here—but space does not permit us to elaborate on this point.

[6] S. H. Vosko, R. Taylor, and G. H. Keech, Can. J. Phys. **43**, 1187 (1965).

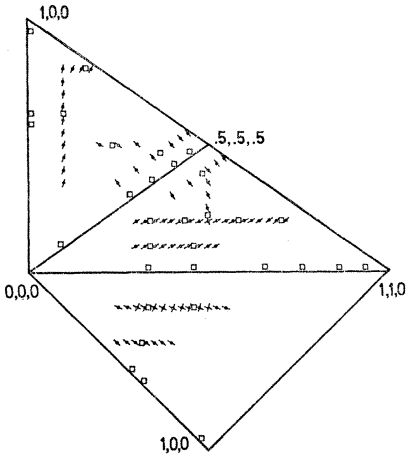

FIG. 2. The sites of measurements not on axes of symmetry (points) and observed anomalies (squares). Dashes through points indicate polarizations of observed phonons.

face, the transition c_1c_3 has weight zero because all translations of the transition vector move one or the other end of it into an empty region. This does not apply to diametrically opposite points near c_1 and c_3. Accordingly, there should be a hole in the associated surface of anomalies at the position corresponding to c, but it is not evident from any simple argument whether or not this hole may be of a size comparable to the resolution of measurements in $\mathbf{q}$ space. The effect is neutralized for phonons with polarization parallel to c_1c_2 because the surface near c_4 acts as a direct continuation of that near c_1 in this case—and likewise for the surfaces near c_2 and c_3.

The screening factor and F' should actually bear the marks of nondiametral transitions as well as diametral. What this may imply for the sizes of the former we do not know, but we assume that the relative sizes for different branches will still be governed by a formula like (2).

The factors in formula (2) are not present in the treatment of anomalies by Taylor.[4] Presumably they disappear or go into disguise when an average value of the matrix element for the electron-phonon interaction in terms of resistivity is introduced in his Eq. (5).

Harrison[7] suggested that the irregularities in the dispersion curves of lead are not images of the Fermi surface, but of the energy–wave-number relation for electrons. In terms of the function F' of Vosko *et al.*[6] which we have utilized above, this means that the observed anomalies might be attributed to the grosser structure, not to the small kink. As Cochran[8] has commented, "it seems unlikely that the rather pronounced kinks in the dispersion curves for lead can be accounted for except in terms of the behavior of the dielectric function"—i.e., in terms of the effect described by Kohn.[1] This comment is borne out by the many details of the present comparison between the Fermi surface and anomalies. But the other effect may give rise to broader humps or dips in dispersion curves; a possible example is mentioned in Sec. 4C.

Maris[9] has suggested that kink-type anomalies in phonon dispersion curves may arise from the phonon-phonon interaction if two of the three phonons involved in one of the simplest types of interaction have the same group velocity. No observed anomalies call for such interpretation, but even from other points of view it seems justifiable to disregard this possibility, in the present instance at least. As in the analogous case of Kohn anomalies, the sharp discontinuity in $\omega(q)$ suggested by the simple consideration of topography [of two different surfaces in $(\mathbf{q},\omega)$ space here] will be "blunted" by several factors in a more complete treatment, and in fact it remains to be proved that an anomaly does occur when these factors have been taken into account. In the first place, the contribution to the phonon energy here involves a sum over states which are not at all so concentrated to a particular neighborhood in wave-vector space as they were in the electron-phonon case: In the electron-phonon case a small shift of $\mathbf{k}$ away from the peak of the interaction's energy resonance entails a relatively large energy shift and large reduction of the interaction probability. Also, the approach to a critical position for an interaction involving three phonons as one moves along a dispersion curve involves the approach to osculation of surfaces $\omega=\omega_2(\mathbf{q})$ and, say, $\omega=\omega_1(\mathbf{q}_1)+\omega_3(\mathbf{q}-\mathbf{q}_1)$, when $\mathbf{q}_1$ varies, and this approach will often be gradual or oblique, as consideration of a two-dimensional example indicates (the subscript 1 here indicates a phonon which interacts virtually with phonons 2 and 3). Moreover, the thickness of dispersion surfaces—the frequency widths of phonons—tends to blur the critical position.

The present section has included a variety of factors that may be involved in irregularities in phonon dispersion curves, and it seems advisable to recapitulate very briefly the more important conclusions for the interpretation of anomalies in lead. The electron transitions corresponding to Kohn anomalies are between points on the Fermi surface where tangent planes are parallel, and may be either diametral or nondiametral. The size and sense of an anomaly depend on the shape of the surface near the points just mentioned, in a way that is amenable to simple qualitative analysis, and the size also depends on three factors contained in formula (2)—the phonon frequency and polarization, and a symmetry factor. In interpreting anomalies, it is appropriate first to attempt an identification of the diametral anomalies listed in Table I, using the expected positions and relative strengths as a rough guide. Then nondiametral transitions may be considered, all the time bearing in mind alterations of previous results necessitated by

[7] W. Harrison, Phys. Rev. **129**, 2512 (1963).
[8] W. Cochran, *Inelastic Scattering of Neutrons* (International Atomic Energy Agency, Vienna, 1965), Vol. I, p. 16.
[9] H. J. Maris, Phys. Letters **22**, 402 (1966).

superpositions. Where anomalies can be followed laterally from symmetry directions, this is of course a valuable aid to identification.

3. OBSERVATION OF ANOMALIES

A general account of our measurements on phonons in lead has been given earlier.[10] A three-axis crystal spectrometer was used to record one-phonon resonances in the inelastic scattering of neutrons by a lead crystal at 80°K, a focusing method being used throughout to optimize resolution. Measurements in the principal symmetry directions were almost everywhere at small enough q intervals to locate anomalies within about 0.02 in q (the unit being 1.279 Å^{-1}, so that reciprocal lattice points have their integral coordinates). Similar detailed series of measurements were made along several other lines in $\mathbf{q}$ space in order to follow the loci of anomalies. The sites of such measurements are indicated in Fig. 2, together with the sites of observed anomalies. The quadrangle in Fig. 2 is the same as in Fig. 1; the polarization of the phonons concerned is indicated by dashes (dashes at right angles indicate that measurements were made on phonons with each polarization).

In looking for anomalies in the phonon dispersion curves of aluminum,[11] we made use of a device for enhancing irregularities, and this was again used here. Corresponding to each dispersion curve or profile (plot of ω along a line in $\mathbf{q}$ space), a curve of $(\Delta\omega/\Delta q)$ versus q along the line was drawn. The values of the slope were taken from pairs of adjacent measurements, and to each value an error was assigned which was a combination of the error estimates for the two measurements concerned. Figure 3 is an example of such a curve for phonons with wave vectors and polarization in the [2,2,0] direction, with a particularly irregular appearance. This treatment of the data reveals anomalies that are often hidden in a curve of ω versus $\mathbf{q}$ by the steep slope. It might seem preferable to remove the effect of large slopes by considering the difference between the observed frequencies and some smooth adjacent curve—among other things, errors would then depend on single measurements, and would not increase as the q interval decreased. But the choice of the smooth curve would require some such analysis of data as our curve of slope versus q involves, and would be arbitrary to an extent that corresponds to errors in the latter curve. So we have kept to the slope analysis. It should be remembered that the errors in a curve such as that in Fig. 3 are not ordinary mutually independent errors: The area under the curve is fixed quite accurately in any interval of, say, 0.2 or longer. In several cases where more than one series of measurements were made, each series was analyzed separately before combining the results, since possible systematic errors do not affect

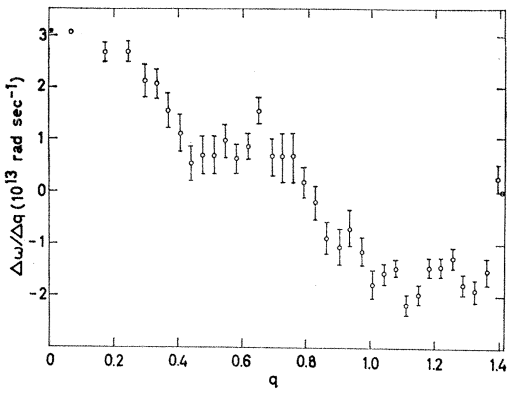

FIG. 3. An example of a curve used in locating anomalies. For phonons with wave vectors and polarization in the [2,2,0] direction.

irregularities in a single series of measurements. Such repeated measurements, as well as measurements at different temperatures and experience from aluminum,[11] indicate that estimated errors in curves like Fig. 3 are too large, but it is difficult to eradicate this error in the errors.

Figure 3 illustrates, though in a rather exceptional fashion, difficulties that may be associated with close juxtaposition of irregularities. From the single curve alone it is not at all obvious whether some anomalies are positive at a certain position or negative at a nearby position. However, information from other curves and successive steps in the construction of a Fermi surface enable such difficulties to be resolved.

4. THE FERMI SURFACE

A. Diametral Transitions

If the picture of the correspondence between anomalies and points on the Fermi surface (FS) is to be convincing, it is hard to avoid tedious detail, but this can be compressed by the use of abbreviations: e.g., "[1,1,1] L No. 2" for "anomaly No. 2 (Table I) in the dispersion curve for L phonons in the [1,1,1] direction"; "the c_1f_3 anomaly" for "the anomaly corresponding to the transition c_1f_3 in Fig. 4."

Numbers 1 and 2 in the [1,1,1] direction do not occur, because the arc from No. 1 in the [2,2,0] direction (e) does not intersect the [1,1,1] axis. No. 3 (b on the FS) is clearly visible, at $q=0.795\pm0.015$. A point near b can be identified in a neighboring profile.

Number 1 in the [2,0,0] direction (h) occurs at $q=0.62\pm0.015$ as a positive anomaly in the L and T branches. This agrees well with other points near e, though since different curvatures occur at h (see Fig. 5) the expected sign is uncertain. An anomaly in a neighboring profile probably corresponds to a point between h and q (near u in Fig. 5). Number 2 (a on the FS) is not immediately apparent. It is very likely that the FS

[10] R. Stedman, L. Almqvist, G. Nilsson, and G. Raunio, Phys. Rev. **163**, 567 (1967).
[11] R. Stedman and G. Nilsson, Phys. Rev. Letters **15**, 634 (1965).

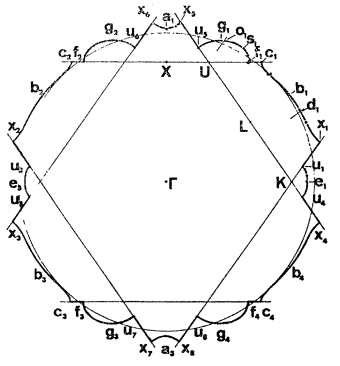

FIG. 4. A section through the Fermi surface. Filled circles indicate points from diametral anomalies, crosses points from nondiametral anomalies. The large circle corresponds to the free-electron sphere.

here is concave outwards, so that the anomaly is negative, and it may then occur (without being obvious) close to No. 1, at $q=0.57\pm0.015$. This assignment is supported by an anomaly in a neighboring profile which corresponds to a point near y. Number 3 disappears if the fourth zone of the FS is empty—and evidence mentioned later shows that this is probably the case. Number 4 is closely connected with Nos. 7 and 9 in the [2,2,0] direction—all three disappear if f_1f_2 is less than 1.414.

Number 1 in the [2,2,0] direction (e) is quite clear at $q=0.455\pm0.015$. Two nearby points in Fig. 4 and two in Fig. 5 may be identified in neighboring profiles. Numbers 2 and 4 are not observed, because the arc from [2,0,0] No. 2(a) does not intersect the [2,2,0] axis. From other observations near b, No. 3 is expected near $q=0.95$; it may be identified with an anomaly at $q=0.94\pm0.02$. Number 5 corresponds to n, and from the estimated positions of h and f is expected at about $q=1.05$; a small positive anomaly in the T_1 branch at $q=1.06\pm0.015$, possibly accompanied by one in the T_2 branch (where large curvature of the dispersion curve makes observation difficult) is the only possibility, and we tentatively assign it to n. Number 6 does not occur if the fourth zone of the FS is empty, and there is no anomaly requiring this assignment. There is no negative anomaly in the L and T_2 branches which could be identified with No. 7, so on this point there is nothing to contradict the conclusion arrived at below, that f_1f_2 is less than 1.414. Marked structure beyond $q=1.1$ in the L and T_1 (Fig. 3) branches may be interpreted in terms of anomalies 8 and 9 (c and f), together with nondiametral anomalies. Number 8 is expected at $q=1.2\pm0.05$: There is a positive anomaly in the L and T_1 branches at $q=1.22\pm0.02$. Number 9 is expected to occur near $q=1.414$: If f_1f_2 is less than 1.414 the anomaly is positive, and vice versa, while if f_1f_2 were exactly 1.414 the anomaly would disappear. c_1f_3 would then correspond to a relatively large negative anomaly near $q=1.31$. The structure suggested by these considerations does actually occur, and leads to $c_1c_2=1.61\pm0.015$, $f_1f_2=1.39\pm0.015$.

B. Nondiametral Transitions

For a near spherical Fermi surface such as that of lead, the main places where pairs of parallel tangent planes may occur are in the same diametral plane, or in the same Bragg plane (taking the Fermi surface to approach Bragg planes perpendicularly) or in parallel planes of one or the other kind. Examination of various nondiametral sections of an approximate Fermi surface indicates that most of the chords that may be significant for anomalies should lie in the diametral planes of Figs. 4 and 5, and this is borne out by the fact that practically all observed anomalies can be accounted for by reference to the two figures concerned. For each figure we may trace anomalies corresponding to transitions between pairs of points with parallel tangent planes that are not diametrically opposite, on the basis of known and estimated features of the Fermi surface. The procedure may be illustrated by reference to Fig. 4: Starting with c_1f_1, a chord with parallel terminations moves in a way that may be described by $c_1f_1\rightarrow x_1s_1$, $x_6s_1\rightarrow a_1g_1\rightarrow x_5u_5$, $x_2u_2\rightarrow c_2e_3$, c_3e_3 (where a comma corresponds to a shift by a reciprocal lattice vector). The locus of the corresponding anomalies may be traced, and it is usually easy to see from the figure what the shape of a given anomaly should be, and in what branch it should be strongest. Another locus of anomalies—as before, for transitions between the second and third zones—is given by $c_3f_1\rightarrow x_3s_1$, $x_8s_1\rightarrow a_3g_1\rightarrow x_7u_5$, $x_4u_2\rightarrow c_4e_3$, c_1e_3, and two for transitions in the third zone are given by $e_1f_1\rightarrow u_1s_1$, $u_6s_1\rightarrow g_2g_1$, etc. and $e_3f_1\rightarrow u_3s_1$, $u_8s_1\rightarrow g_4g_1$, etc. The first and fourth of these loci are smooth curves, while the second and third have sharp bends. The corresponding diagrams for Fig. 5 are particularly simple if the fourth zone of the FS is assumed to be empty, and it is in fact the absence of any anomalies corresponding to the more complicated structure electrons in the fourth zone would entail that is the main argument here for assuming the fourth zone empty.

The loci of anomalies just mentioned must be parts of surfaces on which anomalies may occur. As long as we confine ourselves to symmetry directions the locus curves suffice, but elsewhere we may expect them to be insufficient. For instance, the locus $c_3f_1\rightarrow x_3s_1$, etc. approaches the [1,1,1] axis from one side and then falls back again. This by itself would indicate anomalies near the [1,1,1] axis and on one side of it, but since there is threefold symmetry about the [1,1,1] axis it is quite likely that the locus approaching this axis from one side in the plane of Fig. 4 is actually part of a surface which surrounds the axis and corresponds to anomalies on both sides of it in the plane we are considering. In fact, anomalies do occur on both sides of the [1,1,1] axis in the region concerned, and the only available explanation

seems to be along the lines just mentioned. However, we have not attempted to pursue this explanation in detail.

In the [1,1,1] direction we were previously able to assign only one anomaly, but nondiametral transitions account for four more. A negative anomaly in the L branch at $q=0.15\pm0.015$ corresponds to transitions near c_2f_2. The nearby anomaly expected at $q=0.11$ in the [2,2,0] direction is unfortunately in a region where we have no measurements. A negative anomaly in the L branch at $q=0.27\pm0.015$ corresponds to transitions near x_8u_8. A positive anomaly at $q=0.47\pm0.02$ in the L and T branches corresponds to transitions near u_8s_1. An anomaly in the T branch which may be negative at $q=0.68$ or positive at $q=0.72$, or a combination of both, corresponds to transitions near x_8s_1. This should occur in the L branch too, but is obscured there by the large anomaly at $q=0.8$. In neighboring T_1 profiles there are two associated anomalies, and at (0.26, 0.26, 0.50) in the T_1 branch there is an anomaly [upward towards (0.5, 0.5, 0.5)] corresponding to transitions near x_4u_2.

In the [2,0,0] direction, transitions like g_1g_4 would correspond to an anomaly at about $q=0.38$ in the L branch, but this is not visible, presumably because g is a saddle point. Transitions near a_3h_5 (Fig. 5) may be expected to give negative anomalies near $q=0.97$; in fact both dispersion curves have particularly large curvature at the zone boundary, and this might well be due to nearby negative anomalies.

In the [2,2,0] direction, e_3f_1 would correspond to a positive anomaly in the L and T_1 branches at about $q=0.47$; a weak anomaly in this position is apparent in the T_1 branch, but not in the L branch because of the large negative anomaly at $q=0.46$. Transitions like t_2t_5 would correspond to a positive anomaly in the L branch at about $q=0.5$; it is uncertain whether there is an upward tendency immediately after the negative anomaly at $q=0.46$, but there definitely seem to be juxtaposed negative and positive anomalies at associated positions in neighboring profiles. c_1e_3 would correspond to an anomaly at about $q=0.58$ in the L branch, presumably negative, and nearby transitions to a positive anomaly at about $q=0.63$: It is uncertain whether the negative anomaly occurs, but there is a positive anomaly at $q=0.64\pm0.015$, accompanied by positive anomalies in neighboring profiles (one outside the plane of Fig. 4). e_1f_1 would correspond to an anomaly at about $q=0.92$ in the T_1 branch and g_1g_2 to one at about $q=0.85$ in the L branch, but both would presumably be weak, and they are not in fact discernible. c_1e_1 would correspond to an anomaly in the L branch at about $q=1.03$, but this would also presumably be weak, and is not observed. c_3f_1 corresponds to a negative anomaly in the L and T_1 branches at $q=1.33\pm0.015$, and nearby transitions account for an anomaly in a neighboring profile.

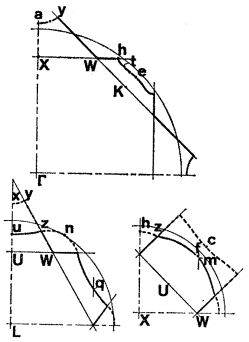

FIG. 5. Partial sections through the Fermi surface. For sections in Bragg planes the surface on both sides of the plane is shown (solid and dashed lines).

C. A Harrison Anomaly?

The only definite irregularity with no apparent explanation in the above terms is a rather broad hump in the T_2 branch at $q=0.57$ in the [2,2,0] direction [$\mathbf{q}=(0.4, 0.4, 0)$], accompanied by similar structure at the nearby point (0.6, 0.4, 0). At 370°K the [2,2,0] T_2 curve has the same shape as at 80°K. The humps have a width of about 0.15 in q. They may perhaps be attributed to a dip in the function $F'(Q)$ at about $Q=1.65$, taking the origin of $\mathbf{Q}$ as (2,0,0) or (0,2,0). A glance at Fig. 21 of Vosko *et al.*[6] shows that $F'(Q)$ may pass through a fairly narrow dip near this position. The site of the dip would be where the curvature is largest, probably just to the left of the minimum. The minimum of F' is a zero which corresponds to a zero of the form factor that enters into the ion-electron element (see, for instance, Vosko *et al.*, Fig. 5, and the associated text).

Examination of the possible sites at which a dip in $F'(Q)$ at about $Q=1.65$ might lead to humps in dispersion curves shows that these would be surprisingly few: (0.35, 0, 0) L, (0.4, 0.4, 0) L and T_2, (0.85, 0.85, 0) L (1.0, 0.7, 0) T_1 and T_2. Of these six, the third is that mentioned above, and conditions for its observation are unusually favorable because the T_2 branch has small curvature in this region. The fifth also seems to occur—near the place where the T_2 branch rises to touch the T_1 branch and polarizations behave in an anomalous fashion (what has been termed "a crossover singularity"), cf. Table I of Ref. 7. The others may occur, but conditions for their observations are not favorable.

If the above interpretation of the observed irregularity is correct, this would be an example of the kind of anomaly suggested by Harrison[7] (see Sec. 2).

D. Results

Figures 4 and 5 are a graphical representation of our results on the Fermi surface. Points from diametral anomalies are shown as filled circles, others by crosses. The uncertainty for the former is mostly about ±0.008, which corresponds to the size of the circles, while for the latter the uncertainty is somewhat greater, since both ends of the transition vector contribute independently in this case. The symbols in the figures coincide with those used by Anderson and Gold,[3] though

TABLE II. Dimensions of the Fermi surface. Our results are compared with those of Anderson and Gold (Ref. 3). The dimensions refer to Figs. 4 and 5.

Dimension	Our value	Anderson and Gold's value
a_1a_3	2.59	2.597
b_1b_3	2.53	2.496
c_1c_2	1.61	1.645
e_1e_3	2.38	2.380
f_1f_2	1.40	1.317
g_1g_4	2.37	2.333
Uu	0.155	0.166
Ux	0.41	
Wn	0.18	0.238
Xh	0.69	0.708

in Fig. 4 suffixes are appended. A smooth Fermi surface has been drawn through the points in each case, and various dimensions of this surface are listed in Table II, together with corresponding dimensions from Anderson and Gold.[3] Where the same dimension has been given in more than one representation by them (in their Table III, $kk=2-hh$, $pp=1-hh$, $vv=1.414+nn$, $ww=1.414-nn$, $\Gamma b=1.732-\frac{1}{2}bb$, $\Gamma e=1.414-\frac{1}{2}ee$), we have included only one. (The value of kk in their Table III implies that k lies outside the free-electron sphere, which does not accord with their Fig. 9, nor with the value they give for hh, and therefore appears to be a misprint.) Some other points are so near to more important points that their positions may be regarded as practically fixed once the more important points are given (d is near b, m near f, o near g, q near u), and these have also been omitted from our table.

Anderson and Gold do not give error estimates for the results we have quoted, but to judge by the errors quoted in their Table I, their uncertainty is of roughly the same order as ours. A general figure for our results is ± 0.007. On this basis it will be seen that there is general fair though not exact agreement between our results and theirs, but poor agreement for f_1f_2 and nn. Even the small differences may be significant, however; for example, their value for b_1b_3 definitely does not agree with the observed anomaly. Their smaller value for f_1f_2 is quite contrary to our observations. Our value for nn is admittedly based on weak evidence, but their value would require an anomaly in the [2,2,0] T_2 branch at a position where nothing can be discerned.

The Fermi surface may be drawn in the form of a series of parallel sections if Figs. 4 and 5 are accepted as in the main accurate. The latter data and the symmetry condition that permutation of the coordinates of a point on the Fermi surface yields another point on the surface determine the whole surface surprisingly well. The volume within our version of the Fermi surface was estimated from such sections and found to be the same as that of the free-electron sphere within 1%, which is within the accuracy of the estimate.

5. THE SIZE OF ANOMALIES

The sizes of anomalies quoted in Table I for a spherical Fermi surface may be expected to apply quite well for [1,1,1] No. 3 and, more roughly, to [2,2,0] Nos. 1 and 3, while elsewhere departures from the spherical shape are large. The observed heights of the respective anomalies are 0.38 ± 0.06, 0.44 ± 0.08, and 0.4 ± 0.1, in units of 10^{13} rad sec^{-1}. When the estimates in Table I are adjusted to take account of the frequencies at the observed sites, and with regard to departures of the Fermi surface from the spherical shape, we find that the sizes in Table I should be multiplied by a factor 3.1 ± 0.3. That is, taking into account the approximate nature of formula (2), $F'(2k_F)=0.031\pm0.005$. The value calculated by Vosko *et al.*[6] (their Fig. 21), based on a one-orthogonalized-plane-wave ion-electron matrix element, is 0.035. Although there is agreement on this point, it should perhaps be pointed out that the shapes of their calculated anomalies are quite different from those observed.

Incidentally, a figure previously given for the size of Kohn anomalies in aluminum[11] may be converted to the same form as above: $F'(2k_F)=0.025\pm0.012$ in aluminum. The value calculated by Vosko *et al.* (their Fig. 17) for a one-orthogonalized-plane-wave matrix element is 0.047 in this case.